TRENDS IN SCIENCES 2026; 23(5): 11753
https://doi.org/10.48048/tis.2026.11753 RESEARCH ARTICLE

Green Synthesized Silver Nanoparticles using *Bauhinia kockiana* Extract Inhibit HeLa Cancer Cells Proliferation and Migratory Ability Via Akt-dependent Pathway

I Gusti Ngurah Agung Wiwekananda[1], Kinar Safira Dyah Paramita[1], To Soon Wei[2], Happy Kurnia Permatasari[3,*], Nik Ahmad Nizam Nik Malek[2,4] and Agustina Tri Endharti[5]

[1]*Biomedical Science Master Program, Faculty of Medicine, Universitas Brawijaya, Malang 65145, Indonesia*
[2]*Department of Biosciences, Faculty of Science, Universiti Teknologi Malaysia, Skudai, Johor 81310, Malaysia*
[3]*Department of Biochemistry and Biomolecular, Faculty of Medicine, Universitas Brawijaya, Malang 65145, Indonesia*
[4]*Centre of Sustainable Nanomaterials, Ibnu Sina Institute for Scientific and Industrial Research, Universiti Teknologi Malaysia, Johor 81310, Malaysia*
[5]*Department of Parasitology, Faculty of Medicine, Universitas Brawijaya, Malang 65145, Indonesia*

([*]Corresponding author's e-mail: happykp@ub.ac.id)

Received: 1 September 2025, Revised: 7 November 2025, Accepted: 17 November 2025, Published: 1 January 2026

Abstract

Cervical cancer remains one of the leading causes of cancer-related mortality among women worldwide, with high-risk HPV infection and dysregulation of the PI3K/Akt signaling pathway playing key roles in its pathogenesis. Current therapeutic strategies are limited by toxicity, resistance, and recurrence, highlighting the need for safer and more effective alternatives. In this study, we explored the potential of silver nanoparticles synthesized via a green approach using *Bauhinia kockiana* leaf extract (BK-AgNPs) as an anticancer agent against HeLa cervical cancer cells. The synthesis of BK-AgNPs was confirmed by UV-Vis spectroscopy, showing surface plasmon resonance peaks at 433 - 443 nm, and particle size analysis revealed an average size of 40 nm with good stability. The anticancer effects of BK-AgNPs were evaluated through scratch assays, In-Cell Western (ICW), and immunofluorescence assays. Results demonstrated that BK-AgNPs inhibited HeLa cell migration significantly compared to the control group, which correlated with reduced expression of phosphorylated Akt (p-Akt), Snail, and Vimentin. These findings suggest that BK-AgNPs exert their effects by generating reactive oxygen species (ROS), leading to inhibition of the PI3K/Akt pathway and suppression of Snail and Vimentin expression, further confirming inhibition of EMT. Collectively, these outcomes demonstrate that BK-AgNPs can effectively impair HeLa cell proliferation and migratory capacity by modulating oncogenic signaling pathways. In conclusion, this study provides evidence that BK-AgNPs synthesized using *B. kockiana* extract represent a promising, environmentally friendly therapeutic approach for cervical cancer, warranting further investigation in preclinical *in vivo* models to validate efficacy and safety.

Keywords: Silver nanoparticles, *Bauhinia kockiana*, Green synthesis, Anticancer, Antimetastasis, Scratch assay, Immunofluorescence, ICW assay, PI3K/AKT

Introduction

Cervical cancer is one of the most prevalent malignancies among females globally, with squamous cell carcinoma being the most frequent histological subtype [1]. In the year 2022, there were 662,301 new cases of cervical cancer recorded worldwide, while 36,964 cases of cervical cancer were recorded in Indonesia. In cases of mortality, cervical cancer is responsible for 348,874 deaths worldwide and 20,708 deaths in Indonesia. Furthermore, cervical cancer is among the top 3 leading cancers, in terms of incidence

and mortality in Indonesia [2]. It is also reported that there is an increased prevalence of cervical cancer in low- to middle-income countries [3]. Various factors are responsible for the development of cervical cancer. However, persistent infection with high-risk strains of Human Papillomavirus (HPV), especially types 16 and 18, besides other HPV strains, is the predominant factor [4]. The overexpression of E6 and E7 oncoproteins derived from high-risk HPV is a crucial factor in the progression of cervical cancer. This is achieved through the dysregulation of the p53 and retinoblastoma (pRb) proteins, respectively, which alters their functionality in regulating the cell cycle [5,6].

Besides degrading p53 and pRb, E6 and E7 interact with various signaling pathways, including the PI3K/Akt pathway, and induce their overactivation [7]. Oncoproteins have the capacity to aberrantly upregulate the PI3K/Akt signaling pathway through either the activation of upstream signaling molecules or mutations in pathway components. This dysregulation leads to the malignant transformation of the infected cells, contributing to genetic instability, dysregulation of proliferation, resistance to apoptosis, enhanced migratory capabilities, and alterations in metabolic properties [8]. Overactivation of the PI3K/Akt pathway also affected its downstream signaling, causing further aberration of cellular signaling and tumor progression in various cancers [9]. Several known downstream targets of Akt are Vimentin [10], which was highly expressed in cervical cancer, and expression was increased with higher grades of tumor [11]. This implication causes the PI3K/Akt signaling pathway to become an essential target for cancer therapy by inhibiting upstream or downstream signaling of this pathway. This could be achieved using an inhibitor agent of this pathway [12].

Surgery during the lower stage of cervical cancer [13], or treatment with chemotherapy and radiotherapy is the most commonly used treatment for cervical cancer [14,15]. Nonetheless, these therapeutic interventions were associated with notable drawbacks, including the recurrence of disease post-operation and patient mortality rates [16]. The occurrence of increased adverse effects and chronic toxicity following chemoradiotherapy treatment has also been documented [17,18]. Research in nanotechnology, particularly concerning the green synthesis of nanoparticles for the treatment, has become a greater research interest over time due to its advantages over conventional cancer therapies. Nanoparticles synthesized through green methods are associated with reduced toxicity and exhibit fewer adverse effects compared to the traditional treatment of cancer [19].

Silver nanoparticles (AgNPs) are one of the nanomaterials that can be synthesized with the green synthesis method and possess potent anticancer properties [20]. Due to their small size, AgNPs can penetrate cancer cells and engage directly with molecular targets. AgNPs also exhibit less toxicity towards healthy cells than cancer cells, making them a promising candidate for safer cervical cancer therapy. The smaller nanoparticle size correlates with an increased surface area-to-volume ratio, significantly enhancing the interaction with cancer cells and facilitating the drug administration process [21,22]. The green synthesis method refers to nanoparticle production using environmentally friendly materials, including plant extracts. These extracts can effectively reduce silver nitrate ($AgNO_3$) to generate AgNPs. Plant extracts are utilized because they eliminate the need for harmful stabilizing or reducing agents during the synthesis of nanoparticles [23]. *Bauhinia kockiana* is a plant whose extracts show significant potential for synthesizing AgNPs, as it contains various beneficial phytochemicals [24]. A prior study indicated that the extract of *B. kockiana* contains several potent anticancer phytochemicals, including gallic acid, methyl gallate, and pyrogallol. Furthermore, it has been shown to inhibit the proliferation of various cancer cell lines [25].

Given the anticancer ability of AgNPs and the plant extract from *B. kockiana*, the green-synthesized AgNPs utilizing this extract (referred to as BK-AgNPs) may emerge as a promising candidate for anticancer therapy. However, there are still very few studies discussing the ability of BK-AgNPs to inhibit cancer proliferation, especially regarding the molecular pathways implicated in this process, which remain limited. Consequently, it is crucial to explore BK-AgNPs as a potential therapeutic agent for cervical cancer, utilizing HeLa cells as a model for cervical cancer. This study is essential for advancing the development of BK-AgNPs as a viable candidate for cancer treatment through the inhibition of Akt, Snail, and vimentin expression.

Materials and methods

Synthesis of AgNPs using *B. kockiana* plant extract

Fresh *B. kockiana* leaves were collected in November 2023 from a private garden in Taman Sri Putri, Skudai, Johor, Malaysia (1.5411°N, 103.6562 °E). The leaves were washed, shade-dried for a week, ground, and sieved (450 µm) into fine powder, then stored in sealed bags at 4 °C. *B. kockiana* leaf extract was prepared by mixing the leaf powder with deionized water, heating for 15 min, and centrifuging at 5,000 rpm for 20 min. The aqueous extract was collected from the separated supernatant. Then, the aqueous silver nitrate ($AgNO_3$) solution was prepared by mixing 0.085g of $AgNO_3$ with 500 mL of deionized water, thus making a stock solution. To synthesize AgNPs, 10 mL of the 1 mM $AgNO_3$ was mixed with 1 mL of 2% *B. kockiana* plant extract and incubated for 24 h for the reduction reaction to occur [26].

Characterization of green synthesized BK-AgNPs

UV-Vis spectroscopy and particle size analysis (PSA) were conducted to confirm the presence and stability of AgNPs resulting from green synthesis using *B. kockiana* plant extract. UV-Vis spectroscopy was performed by aspirating 250 µL of the BK-AgNPs sample into the spectrophotometer cuvette. The cuvette containing the BK-AgNPs sample was then inserted into a Jenway 7,200 Visible spectrophotometer with a 350 - 800 nm wavelength, to perform the UV-Vis analysis. PSA was carried out by vortexing 5 mL of BK-AgNPs for 1 min, then the samples were transferred to a cuvette. The cuvette was subsequently inserted into a SALD-7500nano instrument set at 25 °C for PSA.

HeLa cell culture

HeLa cells were obtained from the Biomedical Laboratory, Faculty of Medicine, Universitas Brawijaya, Malang, East Java, Indonesia. Cells were cultured in Dulbecco's modified Eagle's medium (DMEM) (Invitrogen, Massachusetts), with the addition of 10% Fetal Bovine Serum (FBS) and antibiotics (100 µg/L/mL-penicillin, 100 L/mL Streptomycin) in an incubator at 37 °C and 5% CO_2. The cells were then maintained at pH 7.2 - 7.4 and were routinely harvested with trypsin-EDTA solution [27].

Cell migration assay

Migration ability of HeLa cells was evaluated using the scratch assay. 5×10^4 HeLa cells were seeded in a 24-well plate and incubated for 24 h to allow the cells to proliferate and form a monolayer. A straight line was then scratched at the surface of the well with a yellow micropipette tip and washed with PBS before being treated with different concentrations of BK-AgNPs (20, 40 and 60 ng/mL), except the untreated group. Each well was then observed at 0, 24, and 48 h after treatment using an inverted microscope with 10x magnification. Each well with scratch wounds was visualized and analyzed for quantification using ImageJ software [28].

In-Cell Western (ICW) assay

For the preparation of the ICW assay, 1×10^4 HeLa cells were seeded in a 96-well plate for ICW (LI-COR Biosciences) and incubated for 24 h. Each well was treated with different concentrations of BK-AgNPs (20, 40 and 60 ng/mL), except the untreated group, then incubated for an additional 24 h. Cells in the wells were fixed with 4% paraformaldehyde (PFA) for 20 min at room temperature (20 °C). The cells were then permeabilized with 1% Triton X-100 for 20 min at room temperature and blocked using Intercept® (TBS) Blocking Buffer (LI-COR Biosciences), followed by a 90-minute incubation at room temperature. Cells were then incubated overnight at 4 °C with Rabbit anti-β-actin as a housekeeping gene, Rabbit anti-p-Akt, and Rabbit anti-Vimentin antibodies (Cell Signaling Technology, Inc., MA, USA). All primary antibodies were diluted in a 1:150 ratio. After washing with TBS-Tween four times, cells were incubated with IRDye® 800CW Goat anti-Rabbit IgG Secondary Antibody (1:1,000, LI-COR Biosciences) and CellTag™ 700 Stain (1:500, LI-COR Biosciences) for 1 h at room temperature with gentle agitation. The cells were then rewashed with TBS-Tween four times before being mounted into Odyssey® M (LI-COR Biosciences) for signal detection. Data from microplate scanning were extracted using Empiria Studio® Software version 3.2 [29].

Immunofluorescence assay

1×10^4 HeLa cells were seeded into a 96-well plate for ICW (LI-COR Biosciences) and incubated for 24 h. Each well was then treated with varying concentrations

of BK-AgNPs (20, 40 and 60 ng/mL), except the untreated group. All wells were subsequently incubated for another 24 h. After incubation, all wells are aspirated and washed with 100 µL PBS, then fixed with 4% PFA for 15 min, and washed again with 100 µL PBS before washing further with 0,1% Triton-X 100. All wells are then incubated with 1% bovine serum albumin (BSA) for 5 min, followed by incubation with mouse anti-SNAI1 primary antibody overnight at 4 °C (1:100, Santa Cruz Biotechnology). Nuclear staining performed with DAPI staining (1:1,000, Sigma Aldrich, USA) for 5 min, before observation using Zeiss Confocal Microscope with 400x magnification. Immunofluorescence images are further quantified using ImageJ software [30].

Data collection and statistical analysis

All obtained data were analyzed and presented using the GraphPad Prism 9 application. The data were assessed using the Shapiro-Wilk test to determine the normality of the data and Levene's test to evaluate the homogeneity of the data. Data that fulfill the normality and homogeneity parameters were continued for the one-way analysis of variance (ANOVA) test. The one-way ANOVA was performed to evaluate any significant differences among the various treatment groups ($p < 0.05$). Tukey's HSD post-hoc test determined the significance between each group. The data that did not pass Levene's test were further analyzed with Welch's ANOVA ($p < 0.05$). The analyzed data were illustrated in a diagram.

Results and discussion

***B. kockiana* plant extract successfully synthesizes AgNPs**

This study demonstrated the ability of *B. kockiana* plant extract to act as reducing agents, stabilizers, and capping agents for AgNPs synthesis. After mixing $AgNO_3$ solution with *B. kockiana* plant extract and 24 h of incubation, a dramatic color change with cloudier consistency was observed. This indicates that a reaction occurs during incubation, involving the *B. kockiana* phytochemicals reducing the $AgNO_3$, forming AgNPs (**Figures 1(A)** and **1(B)**). Synthesis of AgNPs using plant extract could be achieved because of the phytochemicals contained in it. The primary mechanism that could be involved in the synthesis process is by reducing the Ag^+ into Ag0 and stabilizing and capping the nanoparticles. This causes AgNPs to form, while maintaining the size around 1 - 100 nm [31]. In this case, previously mentioned phytochemicals such as gallic acid, methyl gallate, and pyrogallol contained in the *B. kockiana* plant extract could be responsible for the synthesis process. Several previous studies that conducted green synthesis of AgNPs also reported a similar change of colour, which, when tested on cancer cell lines, indicated an anticancer ability [32,33].

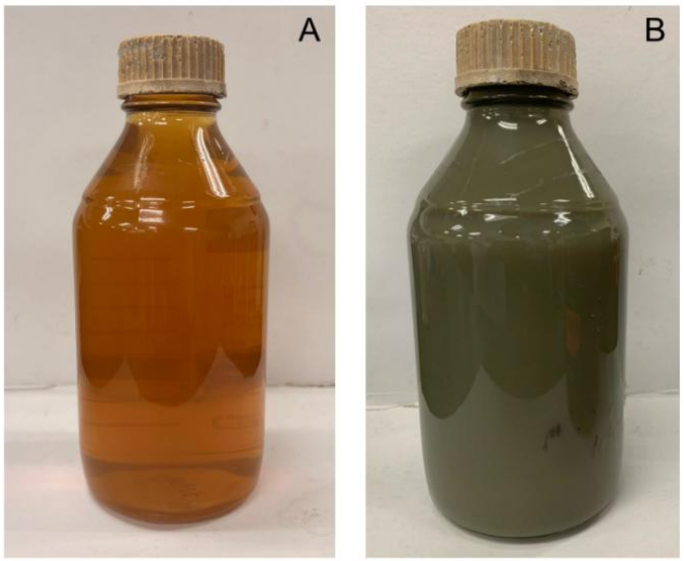

Figure 1 Change of color in the BK-AgNPs. (A) at 0 h, (B) after incubation for 24 h.

Characterization of green synthesized BK-AgNPs

To further confirm the formation of AgNPs using *B. kockiana* plant extract, UV-Vis spectroscopy and PSA were performed, which were later further tested on the HeLa cell line. We also observe the absorbance of UV-Vis periodically to confirm the stability of the AgNPs formed. UV-Vis spectroscopy result indicates the presence of AgNPs after being synthesized using *B. kockiana* plant extract, with the SPR peaks observed around 433 - 443 nm (**Figure 2(A)**). We also observed an increase in absorbance of green synthesized BK-AgNPs in a time-dependent manner, with the absorbance on the sixth day showing the highest absorbance (**Figure 2(B)**). This indicates a high yield of BK-AgNPs with good stability for long-term storage. Successful synthesis of BK-AgNPs was also demonstrated in the particle size results, with an average size of 40 nm and a polydispersity index of 0.525 (**Figure 2(C)**).

UV-Vis spectroscopy and PSA are robust assays to evaluate the AgNPs synthesized using plant extracts. UV-Vis spectroscopy utilizes the unique optical, magnetic, and electrical properties of silver as a metallic material. This analysis will result in a surface plasmon resonance (SPR) peak, which is unique to each material. For AgNPs, SPR peaks usually occur at 380 to 450 nm wavelengths [34]. Compared to the UV-Vis result of this study, it indicates that AgNPs were successfully synthesized since the wavelengths detected were around 380 - 450 nm. Furthermore, UV-Vis spectroscopy is also able to determine the stability of AgNPs periodically, if the SPR peaks are achieved around the same wavelengths tested on different days [35], which was also achieved in this study. This indicates AgNPs were synthesized with good stability and increased in yield each day. The size, shape, morphology, and other properties of AgNPs could also affect the SPR peak formed. Smaller-sized AgNPs often result in the SPR peak being formed at a lower wavelength, while larger-sized AgNPs cause the SPR peak to be formed at a higher wavelength. For example, a previous study reported that AgNPs were formed with a SPR peak at 419 nm wavelength, and the average size of AgNPs was confirmed at 18 nm [36]. This study reported the SPR peaks around 433 - 443 nm with an average size of 40 nm, based on PSA. This confirms the correlation between the SPR peak formed and the size of AgNPs.

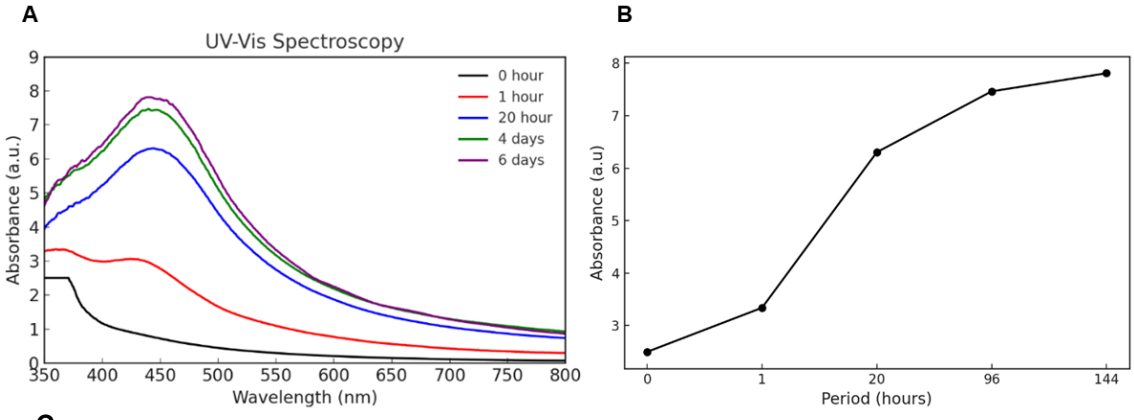

C

Sample Code	Median (nm)	Mean (nm)	Mode (nm)	Standard Deviation (nm)	Absorbance (nm)	Polydispersity Index
AgNP	40	40	32	21	1	0,525

Figure 2 *B. kockiana* plant extract successfully synthesizes AgNPs. (A) UV-Vis spectroscopy results yielding a peak each day of observation, (B) increases in absorbance units of UV-Vis spectroscopy, (C) AgNPs detected with appropriate size and polydispersity index.

BK-AgNPs inhibit HeLa cell migration ability

Synthesized BK-AgNPs were tested on HeLa cells to assess their ability to inhibit cell migration, modeling cervical cancer metastasis. Based on the scratch assay, the results show that BK-AgNPs can reduce the migratory ability of HeLa cancer cells, as evidenced by a wider gap in the BK-AgNPs-treated group compared to the untreated group. A larger gap indicates less migration of HeLa cells to the wounded area, which was inhibited by BK-AgNPs treatment. Even after 48 h, BK-AgNPs treatment consistently resulted in a wider gap compared to the untreated group (**Figure 3**). The inhibition of the migratory ability of HeLa cells involves various interconnected molecular pathways. However, we assume that the PI3K/Akt pathway is one of the main factors that induce the ability of HeLa cells to proliferate and migrate. This could be explained by the cervical cancer itself, which involves E6 and E7 proteins that could interact and overamplify PIK3CA, which in turn, phosphorylates phosphatidylinositol diphosphate (PIP2) to phosphatidylinositol triphosphate (PIP3), which then phosphorylates Akt to p-Akt, causing PI3K-Akt pathway activation [37,38]. p-Akt is able to activate various downstream signaling, including EMT pathways, which are essential modulators in the metastasis of cervical cancer [39]. Based on this notion, inhibition of p-Akt is a key point to inhibit cervical cancer metastasis.

BK-AgNPs could decrease the migration ability of HeLa cancer cells through inhibition of p-Akt by several mechanisms, primarily by reactive oxygen species (ROS) generation. A previous study has reported that some green synthesized AgNPs were able to induce ROS in HeLa cancer cells, which in turn were able to modulate p-Akt and other modulators of metastasis [40]. Other previous study have demonstrated that the AgNPs synthesized using *Citrus hystrix* leaf extract are capable of preventing the migration of HeLa cells to the wound area created using the scratch method [41]. The exact mechanism could be applied in this study, in which BK-AgNPs are able to induce ROS that affects p-Akt, causing inhibition of migratory ability in HeLa cells.

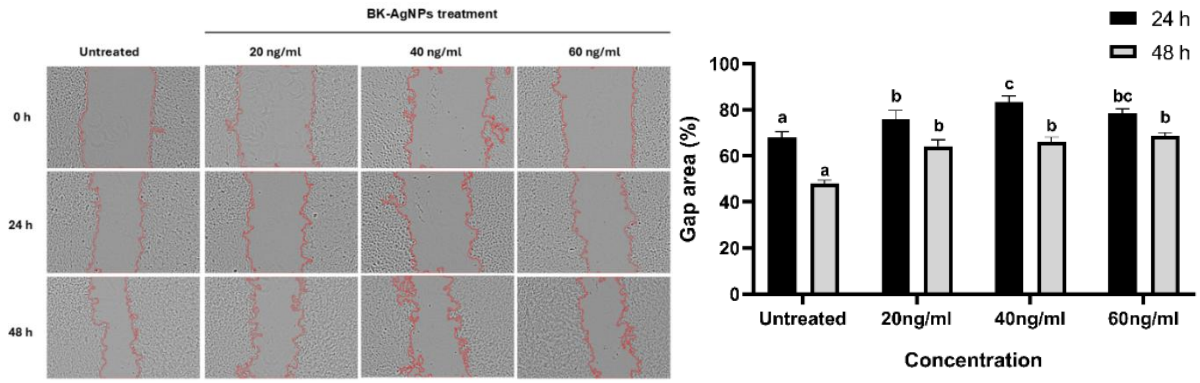

Figure 3 BK-AgNPs inhibit the migratory ability of HeLa cells compared to the untreated group, indicated by the gap area at 0, 24 and 48 h ($p \leq 0.05$).

BK-AgNPs decreased p-Akt expression

The ability of BK-AgNPs to inhibit p-Akt expression was analyzed in this research using the ICW assay. ICW assay has the same principle as western blotting, however, with a plate-based technique that can quantify the fluorescence signal of the targeted protein [42]. **Figure 4** shows ICW assay results on HeLa cells after being treated with BK-AgNPs. Compared to the control group, p-Akt expression was significantly lower in all different BK-AgNPs-treated groups. However, there is a slight, insignificant increase in p-Akt expression in the group treated with 60 ng/mL of BK-AgNPs (**Figure 4**). The decrease in p-Akt expression after BK-AgNPs treatment in this study was mainly caused by ROS generation as the cells were treated with BK-AgNPs, as previously mentioned. ROS could reduce p-Akt expression through several mechanisms, one of which is direct inhibition of p-Akt. AgNPs treatment can induce ROS production, which in turn directly inhibits p-Akt by oxidizing and dephosphorylating it, and hampers downstream signaling [43,44]. Another mechanism involved in p-Akt inhibition is via PTEN, whose role is to dephosphorylate PIP3. ROS presence can enhance

PTEN activity and bind to PIP3, which dephosphorylates it to PIP2. This dephosphorylation causes decreased PIP3 expression, which is required to phosphorylate Akt, which in turn decreases p-Akt expression [45]. This causes reduced activation of the downstream signaling of Akt, which causes decreased migration ability of cancer cells after being treated with BK-AgNPs.

Previous studies have shown that green synthesized AgNPs decrease p-Akt expression by producing ROS, which interacts with the PI3K/Akt pathway. One study using *Gracilaria edulis* marine algae found that AgNPs increased ROS levels in HeLa cells, leading to reduced expression of PI3K, Akt, and mTOR, while also increasing PTEN expression. These findings suggest that AgNPs may affect the PI3K/Akt/mTOR pathway via direct inhibition or modulating PTEN, which in turn interacts with this pathway, resulting in decreased signaling [46]. However, in this study, we observed an increased expression of p-Akt at the highest concentration of BK-AgNPs treatment, although it was not statistically significant compared to the control. This may be caused by excessive ROS production, which in turn activates pro-survival mechanisms in cancer cells, because of their ability to adapt to high ROS levels [47]. Another possible mechanism is the direct oxidation of PTEN if ROS is being excessively produced, particularly by mitochondria. This caused enhanced activity of PI3K/Akt caused by loss of function of PTEN, due to oxidation by ROS [48]. Previous studies have shown that treatment with 5-FU, which exerts its cytotoxic effects on cancer cells mainly through ROS production, leads to elevated ROS levels in 5-FU-resistant CRC cells and simultaneously activates Akt, followed by the activation of HIF-1α [49]. This marks the importance of treatment concentration determination to prevent any adverse results in cancer treatment.

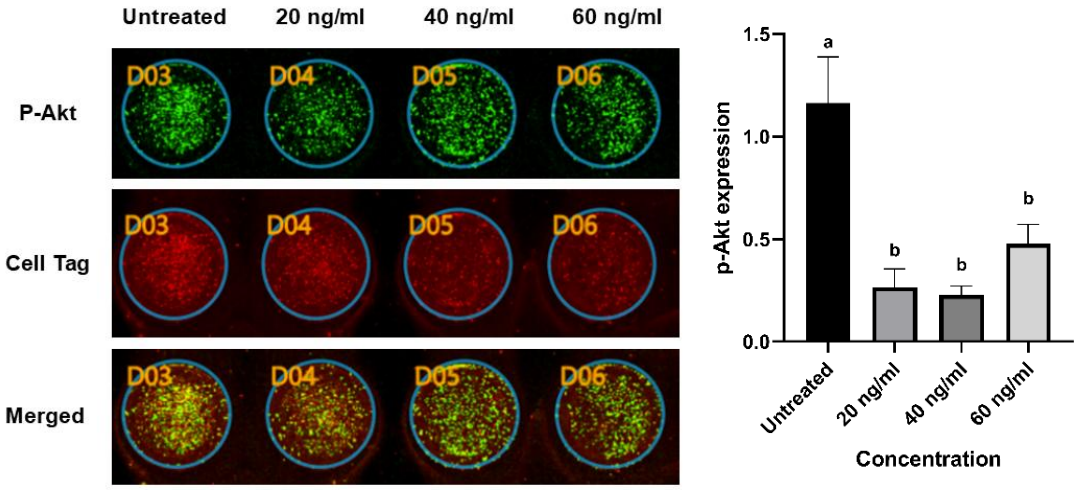

Figure 4 Lower expression of p-Akt in the BK-AgNPs-treated groups compared to the untreated group based on the ICW assay ($p \leq 0.05$).

BK-AgNPs inhibit snail expression

We perform an immunofluorescence assay to observe and quantify Snail expression in HeLa cells after treatment with BK-AgNPs, aiming to understand the mechanism by which BK-AgNPs inhibit HeLa cell migration. The results indicate that BK-AgNPs can inhibit Snail expression in treated groups compared to the untreated group. The findings also show a dose-dependent pattern, with higher concentrations of BK-AgNPs resulting in lower Snail expression (**Figure 5**). Snail is known as a key modulator of epithelial-mesenchymal transition (EMT), which is crucial in the progression of metastasis in various cancers. Snail induces metastasis by upregulating various mesenchymal markers, while downregulating epithelial markers. This causes increased motility and the ability of cancer cells to invade distant tissue and organs [50]. Snail could be regulated by the PI3K/Akt pathway via GSK3β as a bridge between p-Akt and Snail. GSK3β is one of the various downstream signaling pathways of Akt, which are highly phosphorylated during cancer conditions. Phosphorylation of GSK3β causes

phosphorylation of Snail, which in turn activates multiple mesenchymal markers. This causes EMT activation and metastasis progression, initiated by the PI3K/Akt/GSK3β/Snail pathway [9].

Our results show a correlation between p-Akt and Snail expression, with BK-AgNPs treatment reducing p-Akt levels also leading to decreased Snail expression. This reduction in Snail caused by BK-AgNPs, compared to the untreated group, impacts the migratory ability of HeLa cells, as demonstrated using a scratch assay. Similar findings have been reported in previous studies, which indicate that inhibiting the PI3K/Akt/Snail pathway can suppress cancer cell migration [51]. Specifically in green synthesized AgNPs, a previous study has reported that green synthesized AgNPs using *Moringa oleifera* leaf powder could decrease Snail expression in HT-29 human colorectal cancer cells, indicating their antimetastasis ability [52].

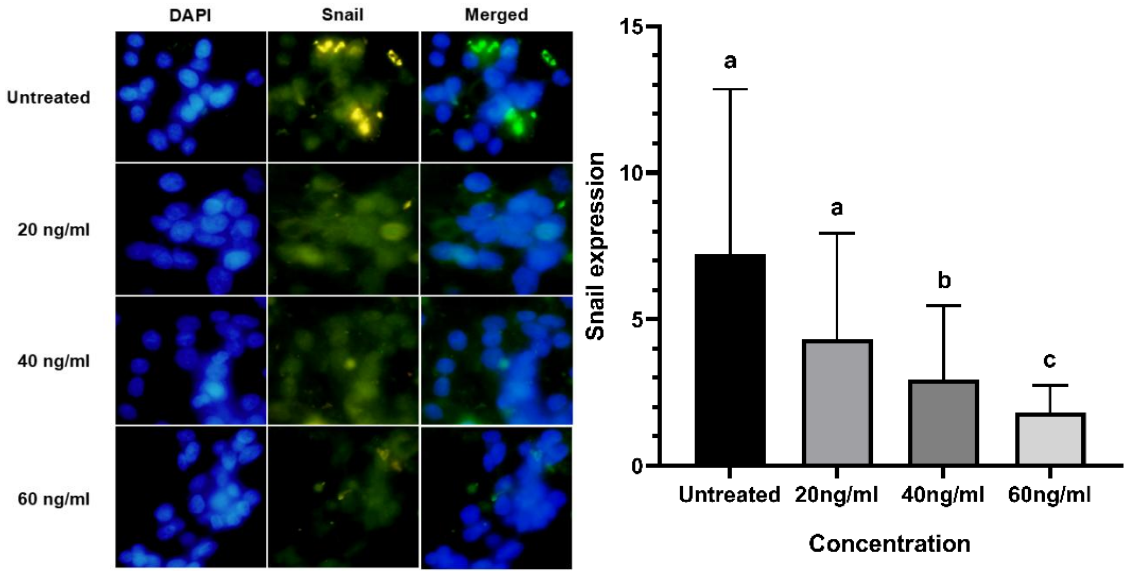

Figure 5 Lower expression of Snail in the BK-AgNPs-treated groups compared to the untreated group based on the immunofluorescence assay ($p \leq 0.05$).

Evaluation of vimentin expression

Using the ICW assay, the expression of Vimentin and after being treated with BK-AgNPs was also evaluated, since there is a correlation between dysregulated Akt and oncogenic pathway, which affects other signaling pathways related to cancer development [12]. **Figure 6** shows that BK-AgNPs treatment significantly reduced Vimentin expression, particularly at a concentration of 40 ng/mL. Similar to p-Akt expression, there is also an increase in Vimentin expression in the group treated with 60 ng/mL of BK-AgNPs (**Figure 6(A)**).

Vimentin is known as one of the essential mesenchymal markers, which is crucial for the development of cancer metastasis by EMT activation. Findings of this study indicate Vimentin expression is affected by p-Akt indirectly, which is by PI3K/Akt/GSK3β/Snail pathway. When Snail are overactivated because of PI3K/Akt dysregulation, they will upregulate various mesenchymal markers, including Vimentin, while downregulating epithelial markers [50]. Vimentin can also be activated directly by Akt, thus increased Akt expression will result in further increases in Vimentin expression [53]. Vimentin then directly regulates various mesenchymal or EMT-related genes, which in turn can be overexpressed and cause increased ability of cancer cells to metastasize to other tissues and organs [54]. This results in reduced expression of Vimentin, which in turn diminishes the ability of cancer cells to migrate and invade other tissues and organs. In this study, this also explains the decreased migratory capacity of HeLa cells treated with BK-AgNPs. Inhibition of Vimentin expression using AgNPs has been reported by previous study that uses AgNPs synthesized using gallic acid [55].

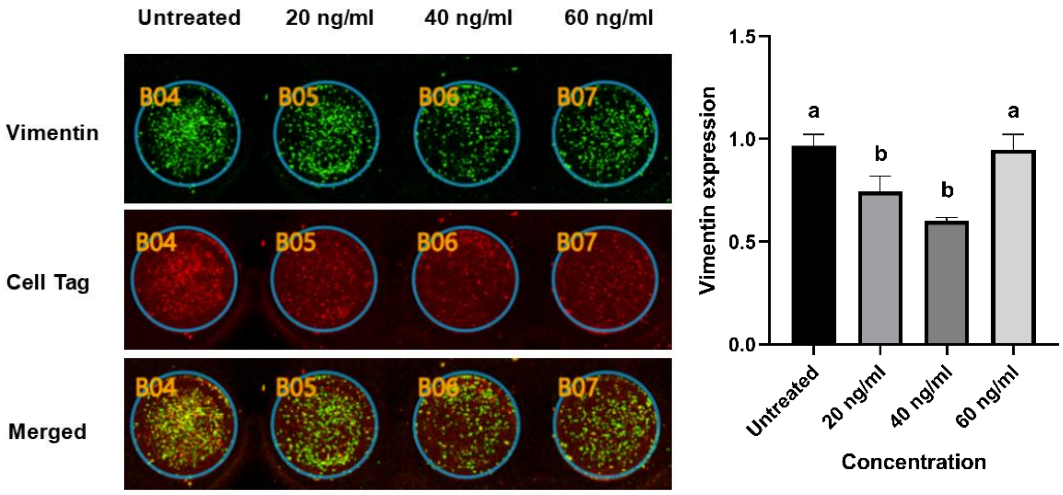

Figure 6 Lower expression of Vimentin in the BK-AgNPs-treated groups compared to the untreated group based on the ICW assay ($p \leq 0.05$).

Conclusions

This study demonstrated the potential of BK-AgNPs as a promising anticancer agent against cervical cancer cells. The green synthesis method using *B. kockiana* plant extract yielded stable nanoparticles with an average size of 40 nm and excellent long-term stability, confirming the role of phytochemicals in facilitating reduction, stabilization, and capping. Functionally, BK-AgNPs significantly inhibited the proliferation and migratory capacity of HeLa cells, through inhibition of HeLa cell migration, which is modelled by the scratch assay. BK-AgNPs are also able to induce the downregulation of the PI3K/Akt pathway, as evidenced by reduced expression of p-Akt, Snail, and Vimentin. These findings emphasize the role of BK-AgNPs in inhibiting HeLa cancer cells, which could be caused by ROS generation after BK-AgNPs treatment. ROS produced after treatment could modulate these pathways by directly interacting with Akt. While the data of this study support the therapeutic potential of BK-AgNPs for cervical cancer treatment, further studies are necessary to confirm these effects *in vivo*, optimize dosing, and evaluate long-term safety. Overall, this research provides new insights into the use of green synthesized nanoparticles as an alternative and potentially safer approach for cervical cancer therapy.

Acknowledgements

The authors acknowledge the Centre of Sustainable Nanomaterials (CSNano), Universiti Teknologi Malaysia, Malaysia, for providing the AgNPs used in this study.

Declaration of Generative AI in Scientific Writing

The authors acknowledge the use of Grammarly® as an AI-assisted language editing tool for grammar and stylistic refinement only. No content generation, data analysis, or interpretation was performed using AI tools. The authors take full responsibility for the content and conclusions of this work.

CRediT Author Statement

I Gusti Ngurah Agung Wiwekananda: Conceptualization; Methodology; Formal analysis; Investigation; Data curation; Writing – original draft; Visualization. **Kinar Safira Dyah Paramita**: Formal analysis; Investigation; Data curation; Writing – original draft; Visualization. **To Soon Wei**: Formal analysis; Investigation; Data curation; Writing – original draft. **Happy Kurnia Permatasari**: Conceptualization; Methodology; Validation; Formal analysis; Resources; Data curation; Writing – review & editing; Visualization; Supervision; Project administration; Funding acquisition. **Nik Ahmad Nizam Nik Malek**: Conceptualization; Methodology; Validation; Resources; Writing – review & editing; Data curation; Supervision; Project administration; Funding acquisition. **Agustina Tri Endharti**: Conceptualization; Validation; Writing - review & editing; Supervision.

References

[1] S Choi, A Ismail, G Pappas-Gogos and S Boussios. HPV and cervical cancer: A review of epidemiology and screening uptake in the UK. *Pathogens* 2023; **12(2)**, 298.

[2] Global Cancer Observatory: Cancer Today, Available at: https://gco.iarc.who.int/today, accessed January 3, 2025.

[3] R Hull, M Mbele, T Makhafola, C Hicks, SM Wang, RM Reis, R Mehrotra, Z Mkhize-Kwitshana, G Kibiki, DO Bates and Z Dlamini. Cervical cancer in low and middle-income countries (Review). *Oncology Letters* 2020; **20(3)**, 2058-2074.

[4] L Schreiberhuber, JE Barrett, J Wang, E Redl, C Herzog, CD Vavourakis, K Sundström, J Dillner and M Widschwendter. Cervical cancer screening using DNA methylation triage in a real-world population. *Nature Medicine* 2024; **30**, 2251-2257.

[5] NNT Sisin, AR Kong, HA Edinur, NIN Jamil and NFC Mat. Silencing E6/E7 oncoproteins in SiHa cells treated with siRNAs and Oroxylum indicum extracts induced apoptosis by upregulating p53/pRb pathways. *Applied Biochemistry and Biotechnology* 2024; **196(7)**, 4234-4255.

[6] INB Mahendra, PKA Prayudi and IBNP Dwija. HPV18 E6/E7 mutation and their association with the expression level of tumor suppressor proteins p53 and pRb among Indonesian women with cervical cancer. *Indonesian Biomedical Journal* 2025; **17(1)**, 51-59.

[7] J Fu, P Yu and Y Liu. Polyphyllin VII inhibits the growth of HPV-positive cervical cancer cells via the PI3K/Akt pathway. *European Journal of Gynaecological Oncology* 2024; **45(6)**, 111-116.

[8] L Zhang, J Wu, MT Ling, L Zhao and KN Zhao. The role of the PI3K/Akt/mTOR signalling pathway in human cancers induced by infection with human papillomaviruses. *Molecular Cancer* 2015; **14**, 87.

[9] S Long, J Wang, F Weng, D Xiang and G Sun. Extracellular matrix protein 1 regulates colorectal cancer cell proliferative, migratory, invasive and epithelial-mesenchymal transition activities through the PI3K/AKT/GSK3β/Snail signaling axis. *Frontiers in Oncology* 2022; **12**, 889159.

[10] QS Zhu, K Rosenblatt, KL Huang, G Lahat, R Brobey, S Bolshakov, T Nguyen, Z Ding, R Belousov, K Bill, X Luo, A Lazar, A Dicker, GB Mills, MC Hung and D Lev. Vimentin is a novel AKT1 target mediating motility and invasion. *Oncogene* 2011; **30(4)**, 457-470.

[11] NEOS Husain, AY Babiker, AS Albutti, MA Alsahli, SM Aly and AH Rahmani. Clinicopathological significance of Vimentin and Cytokeratin protein in the genesis of squamous cell carcinoma of cervix. *Obstetrics and Gynecology International* 2016; **2016**, 8790120.

[12] Y He, MM Sun, GG Zhang, J Yang, KS Chen, WW Xu and B Li. Targeting PI3K/Akt signal transduction for cancer therapy. *Signal Transduction and Targeted Therapy* 2021; **6**, 425.

[13] H Li, Y Pang and X Cheng. Surgery of primary sites for stage IVB cervical cancer patients receiving chemoradiotherapy: A population-based study. *Journal of Gynecologic Oncology* 2020; **31(1)**, 8.

[14] C Chargari, K Peignaux, A Escande, S Renard, C Lafond, A Petit, DLC Kee, C Durdux and C Haie-Méder. Radiotherapy of cervical cancerRadiothérapie des cancers du col utérin. *Cancer/Radiothérapie* 2022; **26(1-2)**, 298-308.

[15] M Liontos, A Kyriazoglou, I Dimitriadis, MA Dimopoulos and A Bamias. Systemic therapy in cervical cancer: 30 years in review. *Critical Reviews in Oncology/Hematology* 2019; **137**, 9-17.

[16] R Nitecki, PT Ramirez, M Frumovitz, KJ Krause, AI Tergas, JD Wright, JA Rauh-Hain and A Melamed. Survival after minimally invasive vs open radical hysterectomy for early-stage cervical cancer: A systematic review and meta-analysis. *JAMA Oncology* 2020; **6(7)**, 1019-1027.

[17] X Yang, Z Li, L Zhang, H Li, XM Yang, Y Sun, L Liu and J Fu. The effect of radiotherapy time and dose on acute hematologic toxicity during concurrent postoperative chemoradiotherapy for early high-risk cervical cancer. *Journal of Cancer* 2023; **14(6)**, 895-902.

[18] BZ Zhang, Y Li, LM Xu, YL Chai, C Qu, YJ Cao, J Wang, HL Hou and J Zhang. The relationship between the radiation dose of pelvic-bone marrow and lymphocytic toxicity in concurrent

chemoradiotherapy for cervical cancer. *Radiation Oncology* 2023; **18(1)**, 12.

[19] IK Karmous, A Pandey, KB Haj and A Chaoui. Efficiency of the green synthesized nanoparticles as new tools in cancer therapy: Insights on plant-based bioengineered nanoparticles, biophysical properties, and anticancer roles. *Biological Trace Element Research* 2020; **196**, 330-342.

[20] N Konappa, RH Patil, AS Kariyappa, S Krishnamurthy, NS Ramachandrappa, R Krishnappa and S Chowdappa. Green synthesis of silver nanoparticles using *Amomum nilgiricum* leaf extracts: Preparation, physicochemical characterization and ameliorative effect against human cancer cell lines. *Cytotechnology* 2025; **77(1)**, 16.

[21] TTH Le, TH Ngo, TH Nguyen, VH Hoang, VH Nguyen and PH Nguyen. Anti-cancer activity of green synthesized silver nanoparticles using *Ardisia gigantifolia* leaf extract against gastric cancer cells. *Biochemical and Biophysical Research Communications* 2023; **661**, 99-107.

[22] A Elmetwalli, MO Abdel-Monem, AH El-Far, GS Ghaith, NAN Albalawi, J Hassan, NF Ismail, T El-Sewedy, MM Alnamshan, NK ALaqeel, IS Al-Dhuayan and MG Hassan. Probiotic-derived silver nanoparticles target mTOR/MMP-9/BCL-2/dependent AMPK activation for hepatic cancer treatment. *Medical Oncology* 2024; **41(5)**, 106.

[23] MB Lava, UM Muddapur, N Basavegowda, SS More and VS More. Characterization, anticancer, antibacterial, anti-diabetic and anti-inflammatory activities of green synthesized silver nanoparticles using *Justica wynaadensis* leaves extract. *Materials Today: Proceedings* 2021; **46(13)**, 5942-5947.

[24] A Pasaribu and K Nurtjahja. Isolation and characterization of flavonoid from leaves of *Bauhinia kockiana* Lour and antibacterial activity. *Journal of Physics: Conference Series* 2020; **1542**, 012045.

[25] YL Chew, YY Lim, J Stanslas, GCL Ee and JK Goh. Bioactivity-guided isolation of anticancer agents from *Bauhinia kockiana* Korth. *African Journal of Traditional, Complementary and Alternative Medicines* 2014; **11(3)**, 291-299.

[26] HK Permatasari, SRA Firdaus, H Susanto, NANN Malek, Widodo, Holipah and HW Sulistomo. Green synthesized moringa oleifera leaf powder - silver nanoparticles (MOLP-AgNPs) promotes apoptosis by targeting Caspase-3 and Phosphorylated-AKT signaling in MCF-7 cells. *Journal of Agriculture and Food Research* 2025; **19**, 101640.

[27] HK Permatasari, ENB Ulfa, VPA Daud, HW Sulistomo and F Nurkolis. *Caulerpa racemosa* extract inhibits HeLa cancer cells migration by altering expression of epithelial-mesenchymal transition proteins. *Frontiers in Chemistry* 2022; **10**, 1052238.

[28] S Yin, H Liu, J Wang, S Feng, Y Chen, Y Shang, X Su and F Si. Osthole induces apoptosis and inhibits proliferation, invasion, and migration of human cervical carcinoma HeLa cells. *Evidence-Based Complementary and Alternative Medicine* 2021; **2021**, 8885093.

[29] Y Kou, S Wang, Y Ma, N Zhang, Z Zhang, Q Liu, Y Mao, R Zhou, D Yi, L Ma, Y Zhang, Q Li, J Wang, J Wang, X Zhou, C He, J Ding, S Cen and X Li. A high throughput cell-based screen assay for LINE-1 ORF1p expression inhibitors using the in-cell western technique. *Frontiers in Pharmacology* 2022; **13**, 881938.

[30] A Bäckström, L Kugel, C Gnann, H Xu, JE Aslan, E Lundberg and C Stadler. A sample preparation protocol for high throughput immunofluorescence of suspension cells on an adherent surface. *Journal of Histochemistry & Cytochemistry* 2020; **68(7)**, 473-489.

[31] CV Restrepo and CC Villa. Synthesis of silver nanoparticles, influence of capping agents, and dependence on size and shape: A review. *Environmental Nanotechnology, Monitoring & Management* 2021; **15**, 100428.

[32] AP Ajaykumar, A Mathew, AP Chandni, SR Varma, KN Jayaraj, O Sabira, VA Rasheed, VS Binitha, TR Swaminathan, VS Basheer, S Giri and S Chatterjee. Green synthesis of silver nanoparticles using the leaf extract of the medicinal plant, *Uvaria narum* and its antibacterial, antiangiogenic, anticancer and catalytic properties. *Antibiotics* 2023; **12(3)**, 564.

[33] J Joseph, KZ Khor, EJ Moses, V Lim, MY Aziz and NA Samad. *In vitro* anticancer effects of *Vernonia amygdalina* leaf extract and green-synthesised silver nanoparticles. *International Journal of Nanomedicine* 2021; **16**, 3599-3612.

[34] NS Alharbi, NS Alsubhi and AI Felimban. Green synthesis of silver nanoparticles using medicinal plants: Characterization and application. *Journal of Radiation Research and Applied Sciences* 2022; **15(3)**, 109-124.

[35] XF Zhang, ZG Liu, W Shen and S Gurunathan. Silver nanoparticles: Synthesis, characterization, properties, applications, and therapeutic approaches. *International Journal of Molecular Sciences* 2016; **17(9)**, 1534.

[36] M Asif, R Yasmin, R Asif, A Ambreen, M Mustafa and S Umbreen. Green synthesis of silver nanoparticles (AgNPs), structural characterization, and their antibacterial potential. *Dose Response* 2022; **20(2)**, 15593258221088709.

[37] A Janecka-Widła, K Majchrzyk, A Mucha-Małecka and B Biesaga. EGFR/PI3K/Akt/mTOR pathway in head and neck squamous cell carcinoma patients with different HPV status. *Polish Journal of Pathology* 2021; **72(4)**, 296-314.

[38] Y Zhang. The effects of PIK3CA mutations on cervical cancer. *E3S Web of Conferences* 2024; **553**, 05025.

[39] Y Chen, S Chen, K Chen, L Ji and S Cui. Magnolol and 5-fluorouracil synergy inhibition of metastasis of cervical cancer cells by targeting PI3K/AKT/mTOR and EMT pathways. *Chinese Herbal Medicines* 2024; **16(1)**, 94-105.

[40] K Kocharyan, S Marutyan, E Nadiryan, M Ginovyan, H Javrushyan, S Marutyan and N Avtandilyan. Royal jelly-mediated silver nanoparticles show promising anticancer effect on HeLa and A549 cells through modulation of the VEGFa/PI3K/Akt/MMP-2 pathway. *Applied Organometallic Chemistry* 2024; **38(12)**, 7726.

[41] S Srimurugan, AK Ravi, VA Arumugam and S Muthukrishnan. Biosynthesis of silver nanoparticles using *Citrus hystrix* leaf extract and evaluation of its anticancer efficacy against HeLa cell line. *Drug Development and Industrial Pharmacy* 2022; **48(9)**, 480-490.

[42] LD Lu and JM Salvino. Chapter Six - The In-Cell Western immunofluorescence assay to monitor PROTAC mediated protein degradation. *Methods in Enzymology* 2023; **681**, 115-153.

[43] Y Liu, C Shi, Z He, F Zhu, M Wang, R He, C Zhao, X Shi, M Zhou, S Pan, Y Gao, X Li and R Qin. Inhibition of PI3K/AKT signaling via ROS regulation is involved in Rhein-induced apoptosis and enhancement of oxaliplatin sensitivity in pancreatic cancer cells. *International Journal of Biological Sciences* 2021; **17(2)**, 589-602.

[44] C Wen, H Wang, X Wu, L He, Q Zhou, F Wang, S Chen, L Huang, J Chen, H Wang, W Ye, W Li, X Yang, H Liu and J Peng. ROS-mediated inactivation of the PI3K/AKT pathway is involved in the antigastric cancer effects of thioredoxin reductase-1 inhibitor chaetocin. *Cell Death & Disease* 2019; **10**, 809.

[45] X Lihui, G Jinming, G Yalin, W Hemeng, W Hao and C Ying. Albicanol inhibits the toxicity of profenofos to grass carp hepatocytes cells through the ROS/PTEN/PI3K/AKT axis. *Fish & Shellfish Immunology* 2022; **120**, 325-336.

[46] N Ravichandran, D Uvarajan, M Ravikumar, K Mahendhran, K Krishnamoorthy, B Vellingiri, C Govindasamy and A Narayanasamy. *Gracilaria edulis*-mediated silver nanoparticles as a targeted strategy for cervical cancer with integrated toxicity evaluation in zebrafish. *Bioorganic Chemistry* 2025; **159**, 108361.

[47] SJ Kim, HS Kim and YR Seo. Understanding of ROS-inducing strategy in anticancer therapy. *Oxidative Medicine and Cellular Longevity* 2019; **2019**, 5381692.

[48] JH Kim, TG Choi, S Park, HR Yun, NNY Nguyen, YH Jo, M Jang, J Kim, J Kim, I Kang, J Ha, MP Murphy, DG Tang and SS Kim. Mitochondrial ROS-derived PTEN oxidation activates PI3K pathway for mTOR-induced myogenic autophagy. *Cell Death and Differentiation* 2018; **25(11)**, 1921-1937.

[49] S Dong, S Liang, Z Cheng, X Zhang, L Luo, L Li, W Zhang, S Li, Q Xu, M Zhong, J Zhu, G Zhang and S Hu. ROS/PI3K/Akt and Wnt/β-catenin signalings activate HIF-1α-induced metabolic reprogramming to impart 5-fluorouracil resistance

in colorectal cancer. *Journal of Experimental & Clinical Cancer Research* 2022; **41(1)**, 15.

[50] Y Huang, W Hong and X Wei. The molecular mechanisms and therapeutic strategies of EMT in tumor progression and metastasis. *Journal of Hematology & Oncology* 2022; **15(1)**, 129.

[51] G Zhang, Z Li, J Dong, W Zhou, Z Zhang, Z Que, X Zhu, Y Xu, N Cao and A Zhao. Acacetin inhibits invasion, migration and TGF-β1-induced EMT of gastric cancer cells through the PI3K/Akt/Snail pathway. *BMC Complementary Medicine and Therapies* 2022; **22(1)**, 10.

[52] H Susanto, SRA Firdaus, M Sholeh, AT Endharti, A Taufiq, NANN Malek and HK Permatasari. *Moringa oleifera* leaf powder - silver nanoparticles (MOLP-AgNPs) efficiently inhibit metastasis and proliferative signaling in HT-29 human colorectal cancer cells. *Journal of Agriculture and Food Research* 2024; **16**, 101149.

[53] R Burikhanov, VM Sviripa, N Hebbar, W Zhang, WJ Layton, A Hamza, CG Zhan, DS Watt, C Liu and VM Rangnekar. Arylquins target vimentin to trigger Par-4 secretion for tumor cell apoptosis. *Nature Chemical Biology volume* 2014; **10(11)**, 924-926.

[54] S Usman, NH Waseem, TKN Nguyen, S Mohsin, A Jamal, MT Teh and A Waseem. Vimentin is at the heart of epithelial mesenchymal transition (EMT) mediated metastasis. *Cancers (Basel)* 2021; **13(19)**, 4985.

[55] SNS Gowda, S Rajasowmiya, V Vadivel, SB Devi, AC Jerald, S Marimuthu and N Devipriya. Gallic acid-coated silver nanoparticle alters the expression of radiation-induced epithelial-mesenchymal transition in non-small lung cancer cells. *Toxicology in Vitro* 2018; **52**, 170-177.